Journal of Organometallic Chemistry 693 (2008) 2415–2423

Contents lists available at ScienceDirect

Journal of Organometallic Chemistry

journal homepage: www.elsevier.com/locate/jorganchem

Isomerization in bent phosphametallocenes: Combining rotational barriers and the intramolecular slip-inversion-slip mechanism to control stereo-conformation

William P. Freeman [b,1], Yi Joon Ahn [b], T. Keith Hollis [a,b,*], J. Andrew Whitaker [a], Victor C. Vargas [b], Ramel J. Rubio [b], Karen D. Alingog [b], Eike B. Bauer [b,2], Fook S. Tham [b]

[a] Department of Chemistry and Biochemistry, 222 Coluter Hall, The University of Mississippi, MS 38677, USA
[b] Department of Chemistry, Physical Sciences 1, University of California, Riverside, CA 92521, USA

ARTICLE INFO

Article history:
Received 9 January 2008
Received in revised form 11 April 2008
Accepted 11 April 2008
Available online 18 April 2008

Keywords:
Phospholyl ring dynamics
Phosphametallocenes
Phosphorus heterocycles
Propylene polymerization

ABSTRACT

Four new phosphazirconocenes, [(4,5,6-trihydro-1-phosphapentalenyl)$_2$ZrCl$_2$] (**8**), [(4,5,6,7-tetrahydro-1-phosphindolyl)$_2$ZrCl$_2$] (**9**), [(4,5,6,7,8-pentahydro-1-phosphazulenyl)$_2$ZrCl$_2$] (**10**), (2,4-dimethylphospholyl)$_2$ZrCl$_2$ (**11**), were prepared and characterized. A crystal structure of [(4,5,6,7-tetrahydro-1-phosphindolyl)$_2$ZrCl$_2$] (**9**), was obtained that revealed disorder (*rac* and *meso* isomers in the same crystal) and demonstrates unambiguously the *meso* configuration in the bent early transition metal phosphametallocenes. Lacking a spectroscopic probe of the rotational dynamics in phosphametallocenes, propylene polymerization was chosen to provide a record of the stereoselective insertions and by inference insight into the phosphametallocene dynamics. Phosphazirconocenes **8**–**11** were evaluated, and the *rac*/*meso* mixture of [(4,5,6,7-tetrahydro-1-phosphindolyl)$_2$ZrCl$_2$] (**9**) was found to produce a mixture of isotactic (iPP) and atactic (aPP) polypropylenes. ^{13}C NMR spectral analysis of the stereo-errors contained in the iPP fraction indicated enantiomorphic site control as the source of the stereoselectivity. The rotational dynamics of the η^5-phospholyl ligand of the parent phosphazirconocene, [(C$_4$H$_4$P)$_2$ZrCl$_2$], was examined as a first order surrogate of reasonable computing complexity for the catalytically active species. The phosphazirconocene was examined using a restricted Hartree–Fock method with a split basis set of 6-311+G(d,p) for C, H, Cl, P and of LANL2DZ for Zr. The rotational potential energy surface was found to be unsymmetrical with a maximum barrier of 8.8 kcal mol^{-1}, which is about an order of magnitude greater than that reported for Cp$_2$ZrCl$_2$. The projection of the calculated rotational dynamics onto a 1-phosphatetrahydroindenyl system is illustrated. This model leads to an interpretation of the polymerization results and the rotational dynamics in phosphametallocenes.

1. Introduction

Having been engaged in the elucidation and applications of early transition metal phosphametallocene dynamics [1], we sought to understand the rotational issues involving the phospholyl ligand. We report herein the synthesis of four new phosphazirconocenes, preliminary polymerization experiments, an initial computational study on the rotational barriers of bent phosphazirconocenes, and a model for interpreting the results.

Numerous studies have been reported describing the rotational barriers of π-ligands in metal complexes [2], and more recently there has been interest in these rotational issues for other heterocyclic π-ligands [3,4]. Metallocene dynamics have been the focus of several groups with recent reports detailing other systems that undergo face-to-face isomerization [5,6]. We have been engaged in a detailed study of the dynamics of bent phosphametallocenes investigating primarily Group 4 (Ti, Zr, Hf) [1,7,8]. In the course of our studies we have reported the slip-inversion-slip mechanism of intramolecular *rac*/*meso* phosphametallocene isomerization and activation parameters associated with certain examples (Scheme 1) [1b,1c].

The slip-inversion-slip mechanism is illustrated in Scheme 2 [1b]. In this mechanism the $\pi(\eta^5)$-bound heterocyclic ligand slips to a $\sigma(\eta^1)$-bound ligand **1** that can then invert at P **2** and ring slip back to the $\pi(\eta^5)$-bound ligand resulting in inversion of the stereochemistry. This process is distinct from the simple rotation around the metal-centroid bond for isomer interconversion, which is also present in phosphametallocenes.

Several groups have reported the use of bent phosphametallocenes as catalysts for olefin polymerization [9]. The development of single-site Ziegler–Natta catalysts for olefin polymerization has

* Corresponding author. Address: Department of Chemistry and Biochemistry, 222 Coluter Hall, The University of Mississippi, MS 38677, USA. Fax: +1 662 915 7301.
E-mail address: hollis@olemiss.edu (T.K. Hollis).
[1] Present address: Nanosys Inc., 2625 Hanover Street, Palo Alto, CA 94304.
[2] Present address: University of Missouri, St. Louis, Department of Chemistry and Biochemistry, One University Boulevard, St. Louis, MO 63121.

0022-328X/$ - see front matter © 2008 Elsevier B.V. All rights reserved.
doi:10.1016/j.jorganchem.2008.04.021

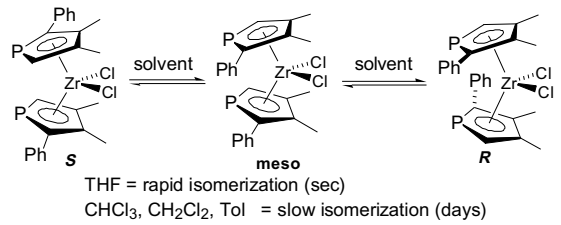

Scheme 1. Isomerization of a phosphazirconocene.

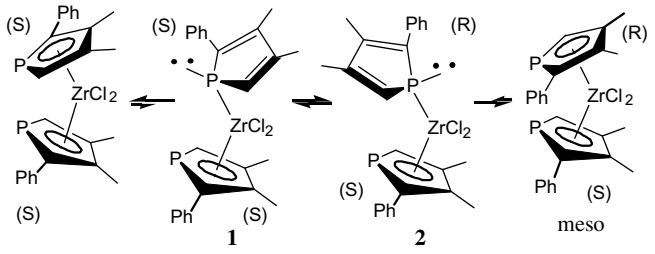

Scheme 2. Slip-inversion-slip mechanism of phosphametallocene interconversion.

been a world-wide, industrial and academic effort [10,11]. A major innovation in this area was the disclosure of ansa-metallocenes as catalysts for the production of isotactic polypropylene (iPP) [11]. The introduction of the "oscillating catalyst" concept sparked considerable work in the area of elastomeric polypropylene (ePP) synthesis (Scheme 3a) [12]. Extensive efforts have been made to manipulate the structures of metallocenes to control the cyclopentadienyl (Cp) rotation rates (k_1, k_{-1}) and thus control the ratio of the stereoblocks [15].

Detailed characterization by high field ^{13}C NMR spectroscopy of the ePP produced by "oscillating catalysts" has revealed a microstructure that differs from that predicted by the Waymouth hypothesis (Scheme 3a) [13]. Busico et al., interpreted the microstructure as a *rac* to *rac* interconversion of the catalyst conformations or a chain-end controlled mechanism, thus avoiding the *meso* conformation and presented a new theory for ePP synthesis (Scheme 3b). While the detailed mechanism of these catalysts is still being debated, achieving a catalyst that fulfills the Waymouth hypothesis will produce a highly-beneficial new class of polypropylene catalysts [14]. As a thermoplastic elastomer, designer ePP would offer many benefits due to its unique properties. Numerous studies have been reported on the synthesis of ePP [15,16]. The key feature of "oscillating catalysts" is control of the rate of catalyst isomerization vs. monomer insertion. These relative rates along with the equilibrium position dictate the microstructure of the polymer (Scheme 3, K_{eq}, k_1, k_{-1}, k_2, k_{-2} vs. k_p^M, k_p^R (or k_p^m, k_p^r)). If a catalyst system can be devised that will accomplish the requirements outline in Scheme 3 a significant advance will be made.

2. Results and discussion

2.1. Synthesis and characterization of phospholes and phosphazirconocenes

The phospholes were synthesized through standard procedures either from commercially-available dienes or easily synthesized dienes (Eq. (1)). Cycloalkanones (**3**, cyclopentanone **3a**, cyclohexanone **3b**, and cycloheptanone **3c**) were reacted with vinyl Grignard [17]. The allylic alcohols obtained were dehydrated with $KHSO_4$ yielding the desired dienes **4a–c** on a gram-scale [18].

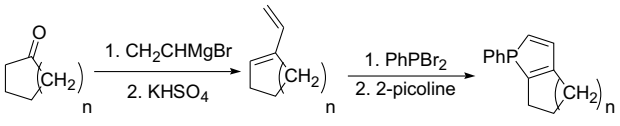

a, n = 1, 13%, 3.6 g
b, n = 2, 19%, 4.6 g
c, n = 3, 5%, 0.4 g

(1)

Phenyl dibromophosphine was prepared according to the literature procedure and employed in the McCormack reaction with each diene to prepare the initial phosphenium heterocycle [9d]. Double dehydrohalogenation of the phosphonium salts with 2-picoline provided the desired phospholes **5a–c** (Eq. (1)) [19]. Commercially obtained 2-methyl-1,3-pentadiene **6** was also subjected to these conditions and produced the desired phosphole **7** (Eq. (2)).

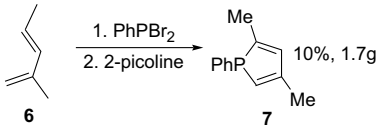

(2)

Standard procedures were employed to prepare the phosphazirconocenes [9b,31]. The phosphole was reacted with Li to cleave the P–Ph bond yielding PhLi and the phospholyl anion. PhLi was quenched with *t*-BuCl, and $ZrCl_4(THF)_2$ was added as illustrated in eq 3. Phosphazirconocenes **8–11** were prepared as outlined in eq 3 and are illustrated below along with the yield of each compound. Phosphazirconocenes **8–11** were obtained as mixtures of *rac* and *meso* isomers as determined by ^{31}P NMR spectroscopy in

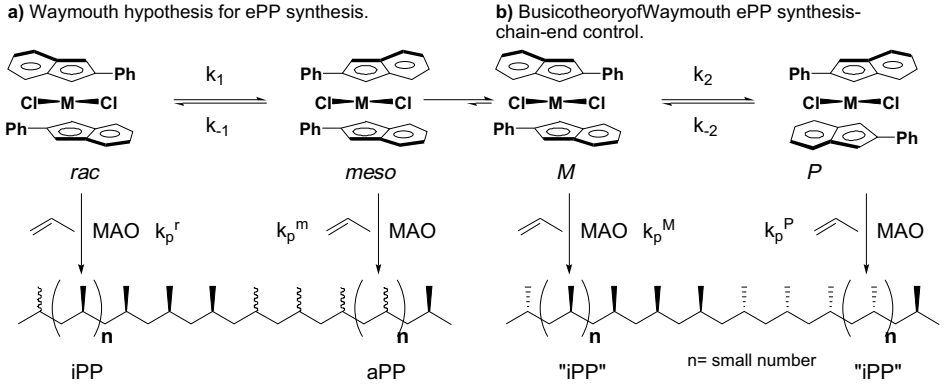

Scheme 3. "Oscillating catalysts" for polypropylene synthesis.

the following ratios: **8** – ~46:54, **9** – initially isolated product: ~46:54; crystalline: ~25:75, **10** – ~50:50, **11** – ~9:91 to ~20:80. Phosphametallocene **8**, $[(P5)_2ZrCl_2]$ (P5 = phosphapentalenyl), was obtained in insufficient quantities for elemental analysis, but the exact mass was found at 405.9137 for a calculated mass of 405.9151. Elemental analyses of phosphametallocenes **9**, $[(P6)_2ZrCl_2]$ (P6 = tetrahydrophosphaindenyl), and **11** – the dimethyl derivative – were consistent with residual ether present as observed in the ^1H NMR spectrum of the compound. Phosphametallocene **10**, $[(P7)_2ZrCl_2]$ (P7 = pentahydrophosphazulenyl), had an elemental composition consistent with that expected.

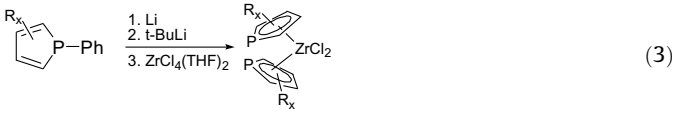

(3)

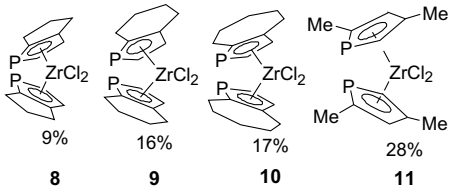

Fractional crystallization of bent phosphametallocenes has been accomplished in several cases [1,7]. All attempts to fractionally crystallize **9** have produced crystals containing a mixture of *rac* and *meso* isomers [20]. An ORTEP plot of the molecular structure in two different perspectives is presented in Fig. 1 along with key metric data for the complex. Although it precluded independent evaluation of the isomers in polymerization, these crystals provide the first reported unambiguous proof of the *meso* isomer in bent phosphametallocenes. Previous structural reports contained only the *rac* isomer. An examination of the racemic isomer depicted in Fig. 1b reveals a staggered array of the phosphazirconocene substituents sterically shields one chlorine (i.e. one site of olefin coordination) more than the other as required for stereoselective polymerization [21]. The details of refinement are included in Table 1.

2.2. Polymerization of propylene with phosphazirconocenes

Phosphazirconocenes **8**–**11** were used as precatalysts for the polymerization experiments. The initially isolated mixtures of diastereomers were evaluated in the polymerization reactions. A simple Fischer–Porter® pressure bottle was employed to condense propylene and conduct the polymerization experiments. Polymerizations were performed employing MAO [Al]/[Zr] 2000:1 at ⩽80 psi of propylene [9]. The polymers from the polymerizations employing precatalysts **8**, **10**, and **11** were entirely soluble in diethyl ether (see supporting information). In contrast, the polymer obtained from precatalyst **9** contained an ether-insoluble (EI) fraction (32%) and an ether-soluble (ES) fraction (68%). GPC of the EI-polymer revealed a M_w/M_n ratio of 1.5. ^{13}C NMR (125 MHz) analysis of the EI fraction revealed an isotactic polymer with 69% *mmmm* pentads and 91% *m* dyads (Fig. 2) [22]. The observed stereo-errors are consistent with the isotactic polymer having been produced by enantiomorphic site control since the *mmmr*, *mmrr*, and *mrrm* pentads have an ~2:2:1 ratio [11b,23]. This observation established the critical fact that the catalyst is responsible for stereocontrol. While the stereoselectivity was modest, it is rare for an unbridged, sterically-uncongested metallocene to have such high levels of stereo-regularity [24,25]. Only complex **9**, $[(P6)_2ZrCl_2]$, produced significant quantities of EI-polymer [26]. An explanation for the observed stereo-regularity is presented below.

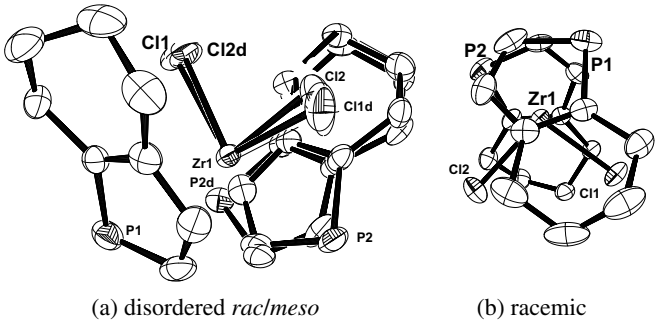

(a) disordered *rac*/*meso* (b) racemic

Fig. 1. (a) ORTEP plot at 50% thermal ellipsoids (hydrogens and centroids omitted for clarity) of one of two disordered molecules in the asymmetric unit cell of phosphazirconocene **9**. The disordered site occupancy ratio is 72/28. (b) View perpendicular to Cl–Zr–Cl plane of the racemic isomer. Selected structural bond distances (Å) and angles (°): Zr1–Ctr1, Ctr2 = 2.270, 2.289, Zr1–Cl1, Cl2 = 2.415(3), 2.443(2), P1–C1 = 1.767(3), P2–C9 = 1.753(5), C1–C2 = 1.384(4), C9–C10 = 1.399(5), Ctr1–Zr1–Ctr2 = 133.55, Cl1–Zr1–Cl2 = 95.9(3), P–Ctr–Zr–Cl = 164.1, 176.4.

Table 1
Crystal data and structure refinement for $[(P6)_2ZrCl_2]$ (**9**)

Empirical formula	$C_{16}H_{20}Cl_2P_2Zr$
Formula weight	436.38
Temperature (K)	218(2)
Wavelength (Å)	0.71073
Crystal system	Monoclinic
Space group	$P2(1)/n$
Unit cell dimensions	
a (Å)	7.4159(7)
b (Å)	24.722(3)
c (Å)	19.0722(17)
α(°)	90
β(°)	92.647(2)
γ (°)	90
Volume (Å^3)	3492.8(6)
Z	8
D_{calc} (Mg/m^3)	1.660
Absorption coefficient (mm^{-1})	1.109
F(000)	1760
Crystal size (mm)	0.36 × 0.24 × 0.05
Θ range for data collection (°)	1.96–28.28
Index ranges	$-9 \leqslant h \leqslant 9$, $-32 \leqslant k \leqslant 32$, $-25 \leqslant l \leqslant 25$
Reflections collected	47 689
Independent reflections [R_{int}]	8661 [0.0411]
Completeness to theta = 28.28°	99.9%
Absorption correction	SADABS
Maximum and minimum transmission	0.9466 and 0.6909
Refinement method	Full-matrix least-squares on F^2
Data/restraints/parameters	8661/1446/618
Goodness-of-fit on F^2	1.078
Final R indices [$I > 2\sigma(I)$]	$R_1 = 0.0291$, $wR_2 = 0.0715$
R indices (all data)	$R_1 = 0.0410$, $wR_2 = 0.0800$
Largest difference peak and hole (e Å^{-3})	0.537 and −0.426

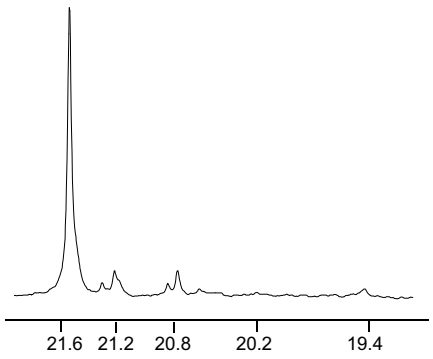

Fig. 2. ^{13}C NMR(125 MHz) of the Me-pentad region of the EI polymer from catalysis with $[(P6)_2ZrCl_2]$ (**9**).

2.3. Phosphametallocene rotational issues: computational study of $(C_4H_4P)_2ZrCl_2$

The rotational barrier in a bent phosphazirconocene pertinent to those in the catalysis reported was evaluated computationally. Geometry optimization and conformational analysis were performed using GAUSSIAN03 at the restricted Hartree–Fock level with a split basis set of 6-311+G(d,p) for C, H, Cl, P and of LANL2DZ for Zr [27]. The initial structure was prepared with the Gaussview graphical interface in the conformation illustrated in Fig. 3, **D**, which is found in most bent phosphametallocene crystal structures. An initial full minimization of the structure was completed at 3-21G* level and used as input for the higher level calculations. This initial conformation was eventually determined to be the global minimum energy structure. This global minimum conformation was chosen to evaluate the rotational potential. One of the phospholyl rings was rotated 10° and a single-point energy calculation was performed. The results of these computations are presented graphically in Fig. 3.

The global minimum-energy conformation is illustrated in Fig. 3 (molecule **D**) along with a plot of the energy vs. rotation angle (α). The presence of two P-atoms produced an unsymmetrical energy surface for rotation of a phospholyl ligand around the metal-centroid axis. The global minimum occurred when the dihedral angle P–Ctr–Zr–Cl angle is ~180° with each P-atom opposite a different Zr–Cl bond (**D**). The next lowest energy minimum has both P-atoms with a dihedral angle of ~180° from the same Cl (**E**) and is 2.1 kcal/mol higher in energy. The other local minimum (Fig. 3, **D**) was 4.5 kcal/mol above the global minimum and occurred when the P-atom bisected the Cl–Zr–Cl angle. The calculations revealed a significant barrier to rotation for $[(C_4H_4P)_2ZrCl_2]$ (Fig. 3). The maximum barrier to rotation of 8.8 kcal/mol occurs when the P eclipses the Zr–Cl bond ($\alpha = 0$). The predicted barrier for $[(C_4H_4P)_2ZrCl_2]$ is an order of magnitude greater than the 1.01 kcal/mol reported for $[Cp_2ZrCl_2]$ [28]. It is also higher than the value reported by Waymouth for indenyl ligands [29], and it is comparable to the neomenthyl-substituted indenyls reported by Erker [30]. Furthermore, the calculated barrier to rotation is on the same scale as monomer insertions in propylene polymerization [13c]. While each rotamer may be accessible under ambient conditions, the Boltzmann distribution predicts the global minimum to be favored 35:1 at 25 °C and ~50:1 at 0 °C vs. the next lowest-energy local minimum. It is well established in X-ray crystal structures that the preferred location of the phosphorous in bent M(IV) phosphametallocenes is the narrow (closed) side of the wedge as illustrated in **D** and **8**–**11**, [1,31] and as may be seen for the structure illustrated in Fig. 1 (*vide supra*). Ring substituents will increase the barrier to rotation and will enhance the preference for the global minimum conformation.

The difference between the barriers in phosphametallocenes and cyclopentadienyl complexes may be seen to arise from the symmetry breaking that occurs upon incorporating the P-atom and the presence of the lone pair on P. The calculated global and local maximum energy conformations **A** and **C** (Fig. 3) occur when the phosphorous and chlorine are eclipsing. The repulsions between the P lone pair and the Cl lone pairs account for the energy increase in phosphametallocenes. Of course, the C–H bond of a cyclopentadienyl ligand will have a significantly reduced repulsion. The global energy minima represented by structure **D** (Fig. 3) may be explained by dipole minimization. In conformation **D**, each P-lone pair vector, and, therefore, local dipole is "anti-parallel" to a Zr–Cl bond dipole vector thus producing a dipole minimum for the molecule.

Phosphametallocene complexes were examined at low temperature. Unsurprisingly, none displayed spectral characteristics that revealed the dynamic nature found in the calculations. At the lowest temperatures observable only one signal for the rapidly interchanging conformations was observed by ^{31}P NMR spectroscopy. It was reasoned that the polymerization studies (*vide supra*) would provide indirect insight into the conformational issues calculated. Propylene polymerizations contain a record of the stereoselectivity of the catalyst [32]. Thus for reactions with enantiomorphic site control the polymer reveals the structure of the catalyst. Therefore, it was reasoned that the phosphametallocene with selectivity in the polymerization provides an indirect record of the conformational structure of the catalyst during polymerization.

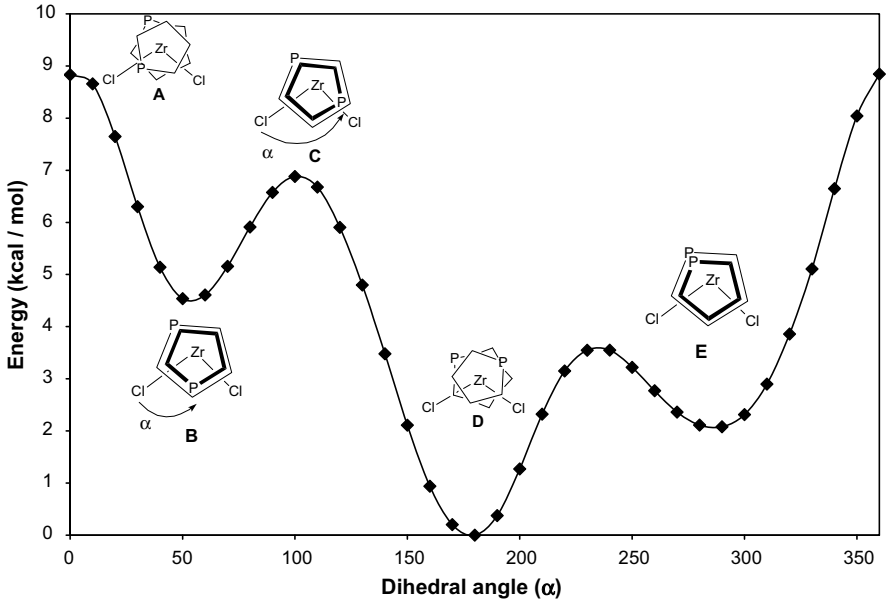

Fig. 3. Energy vs dihedral angle plot for $[(C_4H_4P)_2ZrCl_2]$ calculated at the RHF level with a split basis set with Gaussian03. The basis set for C, H, P, Cl was 6-311+G(d,p), and the basis set for Zr was LANL2DZ. The conformation with the *P*-atom of the top ring eclipsing one of the Zr–Cl bonds is defined as $\alpha = 0$ and rotation toward the other Cl (counterclockwise) is defined as the positive direction.

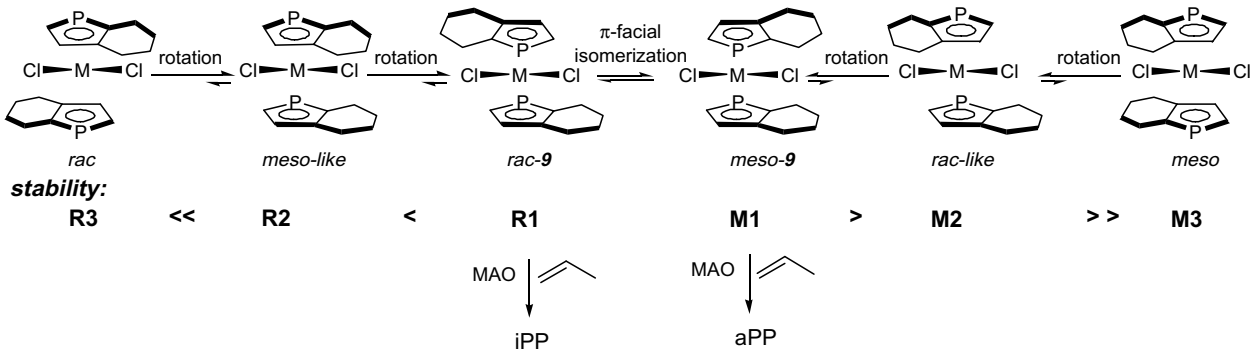

Scheme 4. Rotational and configurational isomers of a chiral bent phosphametallocene.

2.4. Phosphametallocene rotational issues: implications for a substituted phosphametallocene

The conformational analysis of the pre-catalysts, which is a tractable calculation, provides insight into the dynamics of the active form of the catalyst, a much more difficult computational issue. The bent phosphametallocenes have an unsymmetrical energy surface for rotation through 360° unlike Cp-based systems. The consequences of this surface are illustrated for a substituted phosphametallocene relevant to the current study in Scheme 4 [3]. The racemic isomer (**R1**) has two principal conformers of interest at higher energy. There is a "*meso*-like" conformation (**R2**) with one P bisecting the Cl–Zr–Cl angle and a much higher energy "rac" conformation (**R3**) with both P atoms bisecting the Cl–Zr–Cl angle. Likewise, the *meso* isomer (**M1**) has two higher energy conformations - a "*rac*-like" conformation **M2** and a much higher energy "meso" conformation (**M3**) with both P atoms bisecting the Cl–Zr–Cl angle. Thus **R1** and **M1** are expected to be the major conformation present in solution. It is worth noting that in the present situation the barriers to interconversion of the isomers are expected to be greater than the barriers to monomer insertion and polymer propagation, and thus Curtin–Hammett conditions are not obtained [33].

These observations provide a preliminary model for the evaluation of bent phosphametallocenes for polypropylene synthesis. The calculated barrier and preliminary polymerization experiments reported herein are consistent with the expectations of restricted conformational rotation in certain bent phosphametallocenes and a strong preference for the *rac*-conformation **R1** in the chiral configuration and for the *meso* conformation **M1** in the achiral configuration. Simple π-ligand rotation does not produce degenerate energy states as in Cp based systems.

An Occam's razor explanation of the observed polymer fractions is that the *meso* isomer produced the aPP and the *rac* isomer produced the iPP, similar to that reported by Ewen for *ansa*-metallocenes (Scheme 5) [23]. This is consistent with known isomerization rates for phosphametallocenes in non-coordinating solvents [1]. The greater proportion of ES-polymer (68%) is attributed to the *meso*-phosphametallocene **9** in the initially isolated compound (*meso*:*rac*::54:46). These observations are consistent with modest rotational stability and configurational stability of the phosphametallocene on the time scale of monomer insertion (Scheme 5).

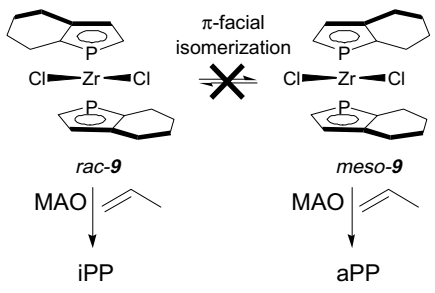

Scheme 5. Rationalization of polymer fractions. Polymerization from depicted conformations was faster than slip-inversion-slip isomerization and rotational interconversion.

3. Conclusions

In conclusion, the introduction of a phosphorous atom into a Cp ring provides a new stereocontrol element for ligand rotation and catalyst development. Several new phosphazirconocenes were evaluated as catalysts for the polymerization of propylene catalysis revealing a precatalyst, [$(P6)_2ZrCl_2$] (**9**), that produced EI-PP, which upon ^{13}C NMR spectral evaluation was isotactic with stereo-errors indicative of enantiomorphic site control. The synthesis of iPP by enantiomorphic site control was consistent with configurational (*rac*/*meso*) stability and modest rotational stability of the phosphazirconocene on the time scale of multiple monomer insertions. While configurational stability was expected based on known isomerization rates [1,7], rotational stability has not been demonstrated previously. A model incorporating configurational and rotational issues is advanced to explain the observations. The relationship between the phosphametallocene *rac*/*meso* isomerization and that of the "oscillating catalysts" is notable. The phosphametallocene "oscillates" (*rac* to *meso*) by a fundamentally different mechanism, which provides alternative methods of controlling the rate (k_1 vs. k_{-1}). These results are consistent with the *rac* isomer **9** producing the iPP and the *meso* isomer **9** producing the aPP. The combined rotational barriers and slip-inversion-slip mechanism suggest an alternate route to achieving the "oscillating catalyst hypothesis" for elastomeric polypropylene (ePP) synthesis. These results suggest that phosphatitanocenes, which have significantly reduced inversion barriers near 11 kcal mol^{-1} may be excellent candidates as catalysts for ePP synthesis [1b].

4. Experimental

4.1. General considerations

All experiments were performed with Schlenk techniques under an atmosphere of Ar or in an Ar filled glovebox. Toluene, THF, CH_2Cl_2 and Et_2O were dried by passing through activated alumina [34]. Pentane was freshly distilled from Na. MAO (Strem®), 2-methyl-1,3-pentadiene (Aldrich®), 2-methylpyridine (Aldrich®), *t*-BuCl (Aldrich®), $MgSO_4$ (EMScience®), HCL (1.0 M EMScience®)

and $ZrCl_4$ (Strem®) were used as received. Propylene (Matheson®) was passed through an O_2 filter before condensation in the polymerization experiments. Phenyl dibromophosphine [35], 1-vinyl-1-cyclopentene [17], 1-vinyl-1-cyclohexene [17] and 1-vinyl-1-cycloheptene [17] were prepared according to the literature procedures. The ^{31}P NMR spectra were calibrated with an external standard 85% H_3PO_4 solution and recorded on Varian® Inova 300 and Inova 500 MHz instruments.

4.2. Preparation of phospholes

Phospholes were prepared according to variations on the literature methods [9d,19].

4.2.1. 1-Phenyl-4,5,6-trihydro-1-phosphapentalene (**5a**)

Phenyl dibromophosphine (38.0 g, 20.2 mL, 142 mmol) and 1-vinyl-1-cyclopentene (26.7 g, 284 mmol) were combined and the flask was placed in the dark. The solution became cloudy after 15 min and after 1 h was opaque. After 2 weeks all volatile components were removed by vacuum transfer. The residue was dissolved in CH_2Cl_2 (120 mL) and added dropwise over 1.5 h to a solution of 2-methyl pyridine (26.4 g, 28.0 mL, 284 mmol) in toluene (200 mL) while the reaction flask was cooled in a water bath. The organic layer was washed with degassed 1.0 M HCl (1 × 100 mL), washed with degassed water (2 × 100 mL), dried over anhydrous magnesium sulfate and filtered. After removal of volatiles the viscous solution was distilled trap to trap. The product was distilled again with a short path distillation apparatus to produce a clear, colorless oil (3.58 g, 17.9 mmol, 13%) with boiling point of 76–78 °C at 0.1 torr. ^1H NMR ($CDCl_3$, 300 MHz): δ 7.42–7.31 (m, 5H), 6.96 (dd, 1H, J_{HH} = 7.5 Hz, J_{PH} = 22.5 Hz), 6.88 (s, 1H), 2.77–2.65 (m, 4H), 2.41–2.32 (m, 2H); ^{13}C {^1H} NMR ($CDCl_3$, 75.5 MHz): δ 156.3 (d, J_{PC} = 13.4 Hz), 148.4 (s), 138.0 (d, J_{PC} = 6.7 Hz), 134.1 (d, J_{PC} = 5.3 Hz), 133.2 (d, J_{PC} = 18.7 Hz), 131.8 (d, J_{PC} = 8.0 Hz), 128.9 (s), 128.7 (d, J_{PC} = 6.7 Hz), 30.7 (s), 30.6 (d, J_{PC} = 6.6 Hz), 28.8 (d, J_{PC} = 5.3 Hz); ^{31}P {^1H} NMR (C_6D_6, 121.5 MHz): δ −6.9 (s).

4.2.2. 1-Phenyl-4,5,6,7-tetrahydro-1-phosphindole (**5b**) [36]

Phenyl dibromophosphine (30.1 g, 16.0 mL, 112 mmol) and 1-vinyl-1-cyclohexene (24.3 g, 225 mmol) were combined and the flask placed in the dark. The solution became cloudy after 15 min and after 1 h was opaque. After 2 weeks all volatile components were removed. CH_2Cl_2 (125 mL) was added and the solution was transferred to a solution of 2-methyl pyridine (26.1 g, 27.6 mL, 280 mmol) in 200 mL of toluene drop-wise over 1.5 h while the reaction flask was cooled in a water bath. The organic layer was washed with degassed 1.0 M HCl (1 × 100 mL) washed with degassed water (2 × 100 mL) dried over anhydrous magnesium sulfate and filtered. After removal of volatiles the viscous solution was distilled trap to trap. The product was distilled again with a short path distillation apparatus to produce a clear colorless oil (4.59 g, 21.4 mmol, 19%) with boiling point of 85–95 °C at 0.1 torr. ^1H NMR (C_6D_6, 300 MHz): δ 7.40–7.35 (m, 2 H), 7.16–7.02 (m, 3H), 6.69 (dd, 1H, J_{PH} = 25.5 Hz, J_{HH} = 7.2 Hz), 6.61 (s, 1H), 2.40–1.92 (m, 4H), 1.47–1.38 (m, 4H); ^{31}P {^1H} NMR (C_6D_6, 121.5 MHz): δ 10.0 (s).

4.2.3. 4,5,6,7,8-Pentahydro-1-phenyl-1-phosphazulene (**5c**)

Phenyl dibromophosphine (11.3 g, 6.0 mL, 42.1 mmol) and 1-vinyl-1-cycloheptene (10.3 g, 84.3 mmol) were combined and the flask placed in the dark. The solution became cloudy after 15 min and after 1 h was opaque. After 2 weeks the volatile components were removed. CH_2Cl_2 (60 mL) was added and the solution was added to a solution of 2-methylpyridine (7.85 g, 8.33 mL, 84.3 mmol) in 100 mL of toluene drop-wise over 1.5 h while the reaction flask was cooled in a water bath. The organic layer was washed with degassed 1.0 M HCl (1 × 100 mL), washed with degassed water (2 × 100 mL), dried over anhydrous magnesium sulfate and filtered. After removal of volatiles the viscous solution was distilled trap to trap. The product was distilled again with a short path distillation apparatus to produce a clear slightly yellow oil (0.422 g, 1.85 mmol, 5%) with boiling point of 85 - 95 °C at 0.1 torr. ^1H NMR ($CDCl_3$, 300 MHz): δ 7.33 (m, 5H), 6.78 (dd, 1H, J_{HH} = 7.2 Hz, J_{PH} = 14.1 Hz), 6.59 (dd, 1H, J_{HH} = 7.2 Hz, J_{PH} = 37.5 Hz), 2.63 (br, 2H), 2.48 (br, 2H), 1.80 (br, 2H), 1.63 (br, 2H), 1.52 (br, 2H); ^{13}C {^1H} NMR ($CDCl_3$, 75.5 MHz): δ 150.9 (d, J_{PC} = 13.6 Hz), 148.**7** (d, J_{PC} = 14.8 Hz), 147.1 (s), 143.7 (d, J_{PC} = 6.7 Hz), 133.9 (d, J_{PC} = 18.7 Hz), 130.9 (d, J_{PC} = 4.7 Hz), 129.4 (s), 128.6 (d, J_{PC} = 8.0 Hz), 32.5 (s), 32.4 (s), 28.8 (*d*, J_{PC} = 21.4 Hz), 28.4 (d, J_{PC} = 5.3 Hz), 27.6 (s); ^{31}P {^1H} NMR (C_6D_6, 121.5 MHz): δ 19 (s).

4.2.4. 2,4-Dimethyl-1-phenyl-phosphole (**7**)

Phenyl dibromophosphine (11.7 g, 43.7 mmol) and 2-methyl-1,3-pentadiene (7.18 g, 87.4 mmol) were combined and the flask placed in the dark. After 2 weeks all volatiles were removed under reduced pressure. CH_2Cl_2 (50 mL) was added and the solution was transferred drop-wise over 1.5 h to a solution of 2-methyl pyridine (8.14 g, 8.60 mL, 87.4 mmol) in toluene (100 mL) while the reaction flask was cooled in a water bath. The organic layer was washed with degassed HCl (1.0 M, 50 mL), washed with degassed water (2 × 50 mL), dried over anhydrous magnesium sulfate and filtered. After removal of volatiles, the viscous liquid was vacuum transferred under reduced pressure. Distillation yielded a pale green oil (1.67 g, 8.88 mmol, 10%), bp = 75–85 °C, 0.1 torr). ^1H NMR ($CDCl_3$, 300 MHz): δ 7.32 (m, 5H), 6.46 (dt, 1H, J_{HH} = 1.5 Hz, J_{PH} = 14.4 Hz), 6.23 (dt, 1H, J_{HH} = 1.5 Hz, J_{PH} = 40.2 Hz), 2.16 (dd, 3H, J_{HH} = 1.2 Hz, J_{PH} = 3.6 Hz), 2.09 (dd, 3H, J_{HH} = 1.2 Hz, J_{PH} = 11.1 Hz); ^{13}C {^1H} NMR ($CDCl_3$, 75.5 MHz): δ 150.8, 149.6 (d, J_{PC} = 8.7 Hz), 136.5 (d, J_{PC} = 10.6 Hz), 133.5 (d, J_{PC} = 20.1 Hz), 132.5 (d, J_{PC} = 9.7 Hz), 129.3, 128.8 (d, J_{PC} = 8.1 Hz), 125.4, 19.3, 15.7 (d, J_{PC} = 20.0 Hz); ^{31}P {^1H} NMR ($CDCl_3$, 121.5 MHz): δ 13.3.

4.3. Preparation of phospholyl complexes [31,9d]

4.3.1. rac- and meso-Bis(4,5,6-trihydro-1-phosphapentalenyl) zirconium dichloride (**8**)

1-Phenyl-4,5,6-trihydro-1-phosphapentalene (1.87 g, 9.35 mmol) was dissolved in THF (40 mL) and Li (0.324 g, 46.8 mmol) was added. The clear, light-yellow–green reaction solution was stirred for 1.5 h and turned opaque brown. The solution was filtered and *t*-BuCl (4.33 g, 5.09 mL, 46.8 mmol) was added and the reaction solution heated at 55 °C for 1 h. During this time the reaction solution turned from opaque brown to clear, light brown. The volatiles were removed and the orange–brown residue was dissolved in Et_2O (60 mL) and added over 15–20 min to $ZrCl_4(THF)_2$ (0.831 g, 2.20 mmol) [37] as a slurry in toluene (15 mL) cooled in a dry ice/ethanol bath. The slurry turned from light-yellow to purple. After 15 min the cooling bath was removed and the solution was allowed to warm to room temperature while stirring overnight. After stirring for 12–14 h at room temperature the solution was cloudy light-yellow with some white precipitate. The volatiles were removed by vacuum transfer and the slightly yellow residue was extracted with Et_2O (3 × 40 mL), the solution was filtered (to remove the extracted portion) and the volatiles were removed by vacuum transfer. The residue was recrystallized from Et_2O/hexane/$(Me_3Si)_2O$ at −35 °C yielding **8** as a yellow solid (0.081 g, 0.199 mmol, 9%). ^1H NMR (C_6D_6, 300 MHz): δ 6.99 (ps dt, *J* = 32.7 Hz, *J* = 12.0 Hz), 6.83 (ps dt, *J* = 31.8 Hz, *J* = 9.3 Hz), 6.30–6.24 (m), 3.30-2.89 (m, 4H), 2.54-2.16 (m, 6H), 1.95–1.84 (m, 2H); ^{13}C {^1H} NMR ($CDCl_3$, 125.774 MHz): 167.6 (d, *J* = 59.1 Hz), 166.0 (ps dt, *J* = 59.1, *J* = 29.0 Hz), 157.5 (s), 157.1 (s), 142.7 (dt, *J* = 59.1 Hz, *J* = 27.0 Hz), 140.4 (ps dt, *J* = 57.1 Hz, *J* = 19.7 Hz),

125.2 (s), 124.3 (d, J = 4.2 Hz), 32.5 (t, J = 13.4 Hz), 32.2 (t, J = 11.3 Hz), 30.2, 30.0, 29.1, 28.9; ^{31}P {^{1}H} NMR (C_6D_6, 121.5 MHz): δ 67.0 (s, 46%), 65.3 (s, 54%). MS (LSIMS): Anal. Calc. for $C_{14}H_{16}Cl_2P_2Zr$: 405.9151. Found: 405.9137. Insufficient sample for elemental analysis.

4.3.2. rac- and meso-Bis(4,5,6,7-tetrahydro-1-phosphindolyl) zirconium dichloride (**9**)

1-Phenyl-4,5,6,7-tetrahydro-1-phosphindole (1.05 g, 4.40 mmol) was dissolved in THF (40 mL) and Li (0.119 g, 17.2 mmol) was added. The clear, light-yellow–green reaction solution was stirred for 1.5 h and turned opaque brown. The solution was filtered to remove lithium. To this solution was added t-BuCl (0.952 g, 1.10 mL, 10.3 mmol), and it was heated at 55 °C for 1 h until the reaction turned from opaque brown to clear, light- brown. The volatiles were removed by vacuum transfer. The orange–brown residue was dissolved in Et_2O (60 mL) and added over 20 min to $ZrCl_4(THF)_2$ (0.831 g, 2.20 mmol) [37] slurried in toluene (15 mL) cooled to −78 °C (dry ice/ethanol). The slurry became red–orange. After 15 min the cooling bath was removed, and the solution was allowed to warm to room temperature while stirring overnight. The solution was cloudy, light-yellow with a white precipitate. The reaction was concentrated, and the slightly yellow residue was extracted with Et_2O (3 × 40 mL), which was filtered and concentrated. The residue was recrystallized in two crops from Et_2O/hexane/$(Me_3Si)_2O$ at −35 °C yielding **9** as a yellow solid (0.305 g, 0.703 mmol, 16%). X-ray quality crystals were grown from Et_2O at −35 °C. ^{1}H NMR (C_6D_6, 300 MHz): δ ^{1}H 6.97 (ps dt, J = 32.7 Hz, J = 10.2 Hz, 2 H), 6.53 (ps dt, J = 31.2, J = 15.9 Hz, 2H), 6.28–6.25 (m, 4H), 3.40–3.06 (m, 8H), 2.58–2.48 (m, 4H), 2.39–2.29 (m, 4H), 1.72–1.62 (m, 8H), 1.43–1.30 (m, 8H); ^{13}C {^{1}H} NMR (C_6D_6, 125.774 MHz): 160.8 (d, J = 56.0 Hz), 159.0 (dt, J = 56.1 Hz, J = 35.2 Hz), 145.6 (s), 144.9 (s), 134.3 (dt, J = 55.0 Hz, J = 31.1 Hz), 133.3 (dd, J = 51.8 Hz, J = 66.4 Hz), 131.9 (s), 130.3 (d, J = 3.1 Hz), 27.8 (t, J = 20.8 Hz), 27.5 (ps t, J = 18.7 Hz), 27.1 (s), 27.0 (s), 22.88 (s), 22.86 (s), 22.0 (s), 21.9 (s); ^{31}P {^{1}H} NMR (C_6D_6, 121.5 MHz): δ 85.4 (s, 46%), 84.4 (s, 54%). MS (LSIMS): Anal. Calc. for $C_{16}H_{20}Cl_2P_2Zr$: 433.9464. Found: 433.9476. Anal. Calc. for $[C_{16}H_{20}Cl_2P_2Zr \cdot 0.33\ C_4H_{10}O]$: C, 45.17; H, 5.10. Found: C, 45.50; H, 4.80%.

4.3.3. rac- and meso-Bis(4,5,6,7,8-pentahydro-1-phosphazulenyl) zirconium dichloride (**10**)

4,5,6,7,8-Pentahydro-1-phenyl-1-phosphazulene (0.422 g, 1.85 mmol) was dissolved in THF (40 mL) and Li (0.064 g, 9.2 mmol) was added. The clear, light-yellow–green reaction solution was stirred for 1.5 h and turned opaque brown. The solution was filtered to remove the lithium. To this solution was added t-BuCl (0.858 g, 1.01 mL, 9.24 mmol) and the reaction was heated at 55 °C for 1 h. The reaction solution turned from opaque brown to clear, light-brown. The reaction was concentrated. The orange–brown residue was dissolved in Et_2O (20 mL) and added over 15–20 min to $ZrCl_4(THF)_2$ (0.349 g, 0.925 mmol) [37] as a slurry in toluene (15 mL) cooled in a dry ice/ethanol bath. The toluene slurry turned from light-yellow to purple. After 15 min the bath was removed and the solution was allowed to warm to room temperature while stirring overnight. After stirring for 12–14 h at room temperature the solution was cloudy light-yellow with some white precipitate. The volatiles were removed, and the slightly yellow residue was extracted with Et_2O (3 × 40 mL). The solution was filtered and the volatiles removed. The residue was recrystallized from Et_2O/hexane/$(Me_3Si)_2O$ at −35 °C yielding **10** as a yellow solid (0.063 g, 0.136 mmol, 17%). ^{1}H NMR (C_6D_6, 300 MHz): δ 6.83 (psuedo dt, J = 31.8 Hz, J = 9.6 Hz, 2 H), 6.59–6.57 (m, 2H), 6.55–6.52 (m, 2H), 6.40 (J = 29.7 Hz, J = 11.4 Hz, 2H), 3.05–2.63 (m, 8H), 1.72–1.57 (m, 6H), 1.39–1.24 (m, 2H), 1.14–0.94 (m, 4H); ^{13}C {^{1}H} NMR ($CDCl_3$, 125.774 MHz): δ 165.4–164.4 (m), 148.8, 148.2, 136.3, 134.9, 132.5 (psuedo dt, J = 54.0 Hz, J = 33.2 Hz), 131.7 (psuedo dt, J = 50.8 Hz, J = 19.7 Hz), 32.9–32.4 (m), 28.4, 28.3, 27.4; ^{31}P {^{1}H} NMR (C_6D_6, 121.5 MHz): δ 96.4 (s, 50%), 93.1 (s, 50%). Anal. Calc. for $C_{18}H_{24}Cl_2P_2Zr$: C, 46.54; H, 5.22. Found: C, 46.46; H, 5.28%.

4.3.4. rac- and meso-Bis(2,4-dimethylphospholyl) zirconium dichloride (**11**)

1-Phenyl-2,4-dimethyl-phosphole (1.01 g, 5.31 mmol) was dissolved in THF (40 mL) and Li (0.129 g, 18.6 mmol) was added. The clear, light-yellow–green reaction solution was stirred for 1.5 h and turned opaque brown. The solution was filtered and to the filtrate t-BuCl (1.48 g, 1.73 mL, 15.9 mmol) was added. The reaction was heated at 55 °C for 30 min. During this time the reaction solution turned from opaque brown to clear, light-brown. The volatiles were removed. The orange–brown residue was dissolved in Et_2O (60 mL) and was added over 15–20 min to $ZrCl_4(THF)_2$ (1.00 g, 2.65 mmol) [37] as a slurry in toluene (15 mL) cooled to −78 °C in a dry ice/ethanol bath. The toluene slurry turned from light-yellow to purple. After 15 min the cooling bath was removed and the solution was allowed to warm to room temperature while stirring overnight. After stirring for 12–14 h at room temperature the solution was cloudy, light green–yellow with a white precipitate. The volatiles were removed by vacuum transfer, and the slightly yellow residue was extracted with Et_2O (3 × 30 mL), filtered, and the volatiles removed by vacuum transfer. The residue was recrystallized from Et_2O/hexane/$(Me_3Si)_2O$ at −35 °C yielding **11** as a yellow solid (0.283 g, 0.742 mmol, 28%). ^{1}H NMR ($CDCl_3$, 300 MHz): δ 7.08–7.01 (m, 2H), 6.97–6.88 (m, 2H), 2.47 (d, 6H, J_{PH} = 9.6 Hz), 2.32 (s, 6H); ^{13}C {^{1}H} NMR ($CDCl_3$, 75.5 MHz): δ 164.3 (d, J = 54.6 Hz), 144.7, 136.6, 135.9, 133.5 (dd, J = 7.7 Hz, J = 59.5 Hz), 19.7, 19.1 (psuedo t, J = 44.4 Hz); ^{31}P {^{1}H} NMR ($CDCl_3$, 121.5 MHz): δ 92.3 (s, 9%), 86.8 (s, 91%). MS (LSIMS): Anal. Calc. for $C_{12}H_{16}P_2Cl_2Zr$: 381.9151. Found: 381.9146. Anal. Calc. for $[C_{12}H_{16}Cl_2P_2Zr \cdot 0.25\ C_4H_{10}O]$: C, 38.76; H, 4.63. Found: C, 38.67; H, 4.50%.

4.4. X-ray structure determination for compound **9**

A yellow fragment of a prism (0.36 × 0.24 × 0.05 mm^3) was used for the single crystal X-ray diffraction study of $C_{16}H_{20}Cl_2P_2Zr$. The crystal was coated with paratone oil and mounted on to a glass fiber. X-ray intensity data were collected at 218(2) K on a Bruker SMART 1000 [38] platform-CCD X-ray diffractometer system (Mo-radiation, λ = 0.71073 Å, 50 kV/45 mA power). The CCD detector was placed at a distance of 4.1770 cm from the crystal. A total of 2424 frames were collected for a hemisphere of reflections (with scan width of 0.3° in ω and ϕ angles of 0°, 90°, 180°, and 270° for every 606, 606, 606, and 606 frames, respectively, 30 s/frame exposure time). The frames were integrated using the Bruker SAINTPLUS software package [39] and using a narrow-frame integration algorithm. Based on a monoclinic crystal system, the integrated frames yielded a total of 47 689 reflections at a maximum 2θ angle of 56.56° (0.75 Å resolution), of which 8661 were independent reflections (R_{int} = 0.0411, R_{sig} = 0.0266, redundancy = 5.5, completeness = 99.9%) and 7160 (82.7%) reflections were greater than $2\sigma(I)$. The unit cell parameters were, a = 7.4159(7) Å, b = 24.722(3) Å, c = 19.0722(17) Å, β = 92.647(2)°, V = 3492.8(6) Å^3, Z = 8, calculated density D_c = 1.109 g/cm^3. Absorption corrections were applied (absorption coefficient μ = 1.109 mm^{-1}; max/min transmission = 0.9466/0.6909) to the raw intensity data using the SADABS program in the SAINTPLUS software [39]. The Bruker SHELXTL (Version 6.10) software package [40] was used for phase determination and structure refinement. The distribution of intensities ($E^2 - 1$ = 0.957) and systematic absent reflections indicated one possible space group; $P2(1)/n$. The space group $P2(1)/n$ was later

determined to be correct. Direct methods of phase determination followed by two Fourier cycles of refinement led to an electron density map from which most of the non-hydrogen atoms were identified in the asymmetry unit of the unit cell. With subsequent isotropic refinement, all of the non-hydrogen atoms were identified. There were two molecules of $C_{16}H_{20}Cl_2P_2Zr$ present in the asymmetry unit of the unit cell. One of the two $C_8H_{10}P$ ligands and the two Cl-atoms coordinated to Zr1 was disordered (disordered site occupancy ratio was 72%/28%). Both the $C_{16}H_{20}P$ ligands coordinated to Zr1′ were disordered (disordered site occupancy ratio was 73%/27%).

Atomic coordinates, isotropic and anisotropic displacement parameters of all the non-hydrogen atoms were refined by means of a full matrix least-squares procedure on F^2. The H-atoms were included in the refinement in calculated positions riding on the atoms to which they were attached. The refinement converged at $R_1 = 0.0291$, $wR_2 = 0.0715$, with intensity, $I > 2\sigma(I)$. The largest peak/hole in the final difference map was 0.537/−0.426 e/Å^3.

4.5. Polymerization

4.5.1. Representative example

A Fischer–Porter® pressure bottle was put under vacuum (~0.1 torr) and back flushed with Ar twice before a final evacuation and filled with propylene. The bottom of the glass bottle was cooled with dry ice/ethanol and 1–2 mL of propylene was condensed as a liquid. The solid co-catalyst methylaluminoxane (MAO) (fwt 58.02 for $[MeAlO]_n$, 0.290 g, 5.0 mmol) was dissolved in toluene (3.5 mL) to produce a clear, straw-yellow solution. The catalyst $(phospholyl)_2ZrCl_2$ (0.0025 mmol) was added and the solution stirred and its color turned to clear light-green–yellow. The precatalyst/co-catalyst mixture was aged 10 min and was injected into the propylene-containing Fischer–Porter bottle.

Once the precatalyst/co-catalyst mixture was added, the dry ice bath was removed and rapid stirring was maintained. The pressure increased and was maintained between 75 and 80 psi in the reaction apparatus. At the desired time the polymerization was stopped by release of the excess propylene and addition of 20 mL of quench solution (3:1 mixture of methanol and 3 N HCl). Toluene (10 mL) was added, the solution stirred in the reaction flask and poured into a separatory funnel. After phase separation of the organic phase the aqueous/methanol phase was extracted with toluene (3 × 10 mL). The organic phases were combined and filtered through a coarse porosity frit. The volatiles were removed and the crude polypropylene was dried under high vacuum (0.1 torr) for at least 8 h.

4.5.2. Fractionation of the polymer

Et_2O (4 mL) was added to the crude polypropylene and the suspension was rapidly stirred for 5–10 min. The polymer was allowed to settle for 30 min. The supernatant was decanted and the extraction process was repeated three times.

4.5.3. Polymer analysis

Polymer samples were analyzed by ^{13}C NMR (125 MHz) in tetrachloroethylene. Molecular weight determinations were made by gel permeation chromatography (GPC) according to the following technique. Molecular weights and molecular weight distributions were measured using a Waters 1500 C gel permeation chromatography equipped with Shodex (Showa Denko) AT-80 M/S columns and a differential refractive index (DRI) detector operating at 145 °C with 1,2,4-trichlorobenzene as the mobile phase at a 1.0 mL/min flow rate. The sample injection volume was 300 mL. The columns were calibrated using narrow polystyrene standards to generate a universal calibration curve. The polypropylene calibration curve was established using $k = 8.33 \times 10^{-5}$ and $a = 0.800$ as the Mark–Houwink coefficients. The numerical analyses were performed using Waters "Millennium" software.

DSC melting points were determined on commercial DSC instruments and are reported as the second melting point. The polymer sample was heated to 200.0 °C for 10 min and then cooled from 200 °C to 25 °C at 10 °C/min. The sample was held at 25 °C for 10 min. The second melt was then recorded as the sample was heated from 25 °C to 200 °C at a rate of 10 °C/min. The peak temperature was recorded as the second melting point.

Acknowledgements

This work was supported in part by NSF Grant CHE-0317089. Acknowledgement is made to the donors of the American Chemical Society Petroleum Research Foundation, the University of California, Cancer Research Coordinating Committee, and the University of California Energy Institute and The University of Mississippi for partial support of this work. Y.J.A. and R.J.R. acknowledge support from the Department of Education, GAANN program. The authors thank Dr. Richard Kondrat and Mr. Ron New for mass spectral analyses and Dr. Dan Borchardt for assistance with NMR analyses. We gratefully acknowledge Dr. Terry Burkhardt of ExxonMobil for performing the GPC and DSC analyses of the polymers.

Appendix A. Supplementary material

CCDC 252898 contains the supplementary crystallographic data for **9**. These data can be obtained free of charge from The Cambridge Crystallographic Data Centre via www.ccdc.cam.ac.uk/data_request/cif. Supplementary data associated with this article can be found, in the online version, at doi:10.1016/j.jorganchem.2008.04.021.

References

[1] (a) T.K. Hollis, Y.J. Ahn, F.S. Tham, Organometallics 22 (2003) 1432;
(b) T.K. Hollis, Y.J. Ahn, F.S. Tham, Chem. Commun. (2002) 2996;
(c) Y.J. Ahn, R.J. Rubio, T.K. Hollis, F.S. Tham, B. Donnadieu, Organometallics 25 (2006) 1079.
[2] (a) For leading references see: W.D. Luke, A. Streitwieser, J. Am. Chem. Soc. 103 (1981) 3241;
(b) C.H. Winter, D.A. Dobbs, X.X. Zhou, J. Organomet. Chem. 403 (1991) 145;
(c) S. Carter, J.N. Murrell, J. Organomet. Chem. 192 (1980) 399;
(d) W.W. Lukens Jr., S.M. Beshouri, A.L. Stuart, R.A. Andersen, Organometallics 18 (1999) 1247;
(e) J.S. Waugh, J.H. Loehlin, F.A. Cotton, D.P. Shoemaker, J. Chem. Phys. 31 (1959) 1434;
(f) C.H. Winter, X.X. Zhou, M.J. Heeg, Inorg. Chem. 31 (1992) 1808;
(g) E. Maverick, J.D. Dunitz, Mol. Phys. 62 (1987) 451.
[3] For heterocyclic π-ligands see: M. Ogasawara, K. Yoshida, T. Hayashi, Organometallics 22 (2003) 1783.
[4] J.M. Tanski, G. Parkin, Organometallics 21 (2002) 587.
[5] (a) F.G.N. Cloke, K.R. Flower, C. Jones, R.M. Matos, J.F. Nixon, J. Organomet. Chem. 487 (1995) C21;
(b) F.W. Heinemann, H. Pritzkow, M. Zeller, U. Zenneck, Organometallics 19 (2000) 4283;
(c) F.W. Heinemann, H. Pritzkow, M. Zeller, U. Zenneck, Organometallics 20 (2001) 2905;
(d) F.W. Heinemann, M. Zeller, U. Zenneck, Organometallics 23 (2004) 1689.
[6] (a) O.J. Curnow, G.M. Fern, M.L. Hamilton, A. Zahl, R. van Eldik, Organometallics 23 (2004) 906;
(b) O.J. Curnow, G.M. Fern, Organometallics 21 (2002) 2827;
(c) O.J. Curnow, G.M. Fern, M.L. Hamilton, E.M. Jenkins, J. Organomet. Chem. 689 (2004) 1897.
[7] For related work see: S. Bellemin-Laponnaz, M.M.C. Lo, T.H. Peterson, J.M. Allen, G.C. Fu, Organometallics 20 (2001) 3453.
[8] (a) For recent reviews of phosphametallocenes see: F. Mathey, J. Organomet. Chem. 646 (2002) 15;
(b) C. Ganter, J. Chem. Soc., Dalton Trans. (2001) 3541;
(c) F. Mathey, Coord. Chem. Rev. 137 (1994) 1.
[9] (a) C. Janiak, K.C.H. Lange, P. Marquardt, J. Mol. Cat. A: Chem. 180 (2002) 43;
(b) C. Janiak, K.C.H. Lange, U. Bersteeg, D. Lentz, P.H.M. Budzelaar, Chem. Ber. 129 (1996) 1517;
(c) C. Janiak, U. Versteeg, K.C.H. Lange, R. Weimann, E. Hahn, J. Organomet.

Chem. 501 (1995) 219;
(d) E.J.M. de Boer, I.J. Gilmore, F.M. Korndorffer, A.D. Horton, A. van der Linden, B.W. Royan, B.J. Ruisch, L. Schoon, R.W. Shaw, J. Mol. Catal. A: Chem. 128 (1998) 155;
(e) S.J. Brown, X. Gao, D.G. Harrison, L. Koch, R.E.v.H. Spence, G.P.A. Yap, Organometallics 17 (1998) 5445.
[10] (a) K. Ziegler, E. Holzkamp, H. Breil, H. Martin, Angew. Chem. 67 (1955) 541;
(b) G. Natta, P. Pino, P. Corradini, F. Danusso, E. Mantica, G. Mazzanti, G. Moraglio, J. Am. Chem. Soc. 77 (1955) 1708.
[11] (a) For recent reviews: special issue: Chem. Rev. 2000 100 (4).;
(b) H.H. Brintzinger, D. Fischer, R. Mulhaupt, B. Rieger, R.M. Waymouth, Angew. Chem., Int. Ed. Engl. 34 (1995) 1143. and references therein;
(c) R.L. Halterman, Chem. Rev. 92 (1992) 965.
[12] G.W. Coates, R.M. Waymouth, Science (Washington, DC) 267 (1995) 217.
[13] (a) V. Busico, R. Cipullo, G. Talarico, V. Van Axel Castelli, Isr. J. Chem. 42 (2003) 295;
(b) V. Busico, V.V.A. Castelli, P. Aprea, R. Cipullo, A. Segre, G. Talarico, M. Vacatello, J. Am. Chem. Soc. 125 (2003) 5451;
(c) V. Busico, R. Cipullo, W.P. Kretschmer, G. Talarico, M. Vacatello, V.V. Castelli, Angew. Chem., Int. Ed. Engl. 41 (2002) 505.
[14] V. Busico, R. Cipullo, W. Kretschmer, G. Talarico, M. Vacatello, V.V. Castelli, Macromol. Symp. 189 (2002) 127.
[15] (a) W. Wiyatno, Z.R. Chen, Y.X. Liu, R.M. Waymouth, V. Krukonis, K. Brennan, Macromolecules 37 (2004) 701;
(b) J.L.M. Petoff, M.D. Bruce, R.M. Waymouth, A. Masood, T.K. Lal, R.W. Quan, S.J. Behrend, Organometallics 16 (1997) 5909;
(c) M.D. Bruce, G.W. Coates, E. Hauptman, R.M. Waymouth, J.W. Ziller, J. Am. Chem. Soc. 119 (1997) 11174;
(d) C.D. Tagge, R.L. Kravchenko, T.K. Lal, R.M. Waymouth, Organometallics 18 (1999) 380;
(e) P. Witte, T. Lal, R. Waymouth, Organometallics 18 (1999) 4147;
(f) S. Lin, R.M. Waymouth, Macromolecules 32 (1999) 8283;
(g) J.L.M. Petoff, C.L. Myers, R.M. Waymouth, Macromolecules 32 (1999) 7984;
(h) M. Nele, S. Collins, M.L. Dias, J.C. Pinto, S. Lin, R.M. Waymouth, Macromolecules 33 (2000) 7249;
(i) S. Lin, C.D. Tagge, R.M. Waymouth, M. Nele, S. Collins, J.C. Pinto, J. Am. Chem. Soc. 122 (2000) 11275;
(j) S. Lin, R. Kravchenko, R.M. Waymouth, J. Mol. Cat. A: Chem. 158 (2000) 423;
(k) R. Schmidt, H.G. Alt, J. Organomet. Chem. 621 (2001) 304.
[16] (a) T. Dreier, G. Erker, Isr. J. Chem. 42 (2002) 343;
(b) T. Dreier, G. Erker, R. Frohlich, B. Wibbeling, Organometallics 19 (2000) 4095;
(c) E. Polo, S. Losio, F. Fortini, P. Locatelli, M.C. Sacchi, Macromol. Symp. 213 (2004) 89.
[17] W. Herz, R.R. Juo, J. Org. Chem. 50 (1985) 618.
[18] P.A. Robins, J. Walker, J. Chem. Soc. (1952) 642.
[19] A. Breque, F. Mathey, P. Savignac, Synthesis (1981) 983.
[20] Crystal data for **9**: $C_{16}H_{20}Cl_2P_2Zr$, $M_w = 436.38$, monoclinic, $P2(1)/n$, $a = 7.4159(7)$, $b = 24.722(3)$, $c = 19.0722(17)$ Å, $V = 3492.8(6)$ Å^3, $Z = 8$, $d = 1.660$ g cm^{-3}, $T = 218(2)$ K, $R = 0.0410$, $wR_2 = 0.0800$, GOF = 1.078. CCDC 252898 (**1**) contains the supplementary crystallographic data for this paper. These data can be obtained free of charge via www.ccdc.cam.ac.uk/conts/retrieving.html (or from the Cambridge Crystallographic Data Centre, 12, Union Road, Cambridge CB2 1EK, UK; fax: (+44) 1223-336-033; or deposit@ccdc.cam.ac.uk).
[21] G.W. Coates, Chem. Rev. 100 (2000) 1223.
[22] V. Busico, R. Cipullo, G. Monaco, M. Vacatello, A.L. Segre, Macromolecules 30 (1997) 6251.
[23] J.A. Ewen, J. Am. Chem. Soc. 106 (1984) 6355.
[24] For an example at low temperature see: Ref. 23. For a sterically congested example see: G. Erker, M. Aulbach, M. Knickmeier, D. Wingbermuhle, C. Kruger, M. Nolte, S. Werner, J. Am. Chem. Soc. 115 (1993) 4590.
[25] (a) Bis(indenyl)$ZrCl_2$ and bis(tetrahydroindenyl)$ZrCl_2$ produce aPP: M.R. Meneghetti, M.C. Forte, J. Dupont, Polym. Bull. (Berl.) 35 (1995) 431;
(b) E. Polo, S. Losio, F. Forlini, P. Locatelli, A. Provasoli, M.C. Sacchi, Macromol. Chem. Phys. 203 (2002) 1859.
[26] (a) For another example of fused ring size making a difference in stereoselectivity see: J.A. Ewen, R.L. Jones, M.J. Elder, in: W. Kaminsky (Ed.), Expanding the Scope of Metallocene Catalysis: Beyond Indenyl and Fluorenyl Derivatives, Springer-Verlag, New York, 1999, pp. 150–169;
(b) J.A. Ewen, R.L. Jones, M.J. Elder, A.L. Rheingold, L.M. Liable-Sands, J. Am. Chem. Soc. 120 (1998) 10786.
[27] M.J. Frisch, G.W. Trucks, H.B. Schlegel, G.E. Scuseria, M.A. Robb, J.R. Cheeseman, J.A. Montgomery, Jr., T. Vreven, K.N. Kudin, J.C. Burant, J.M. Millam, S.S. Iyengar, J. Tomasi, V. Barone, B. Mennucci, M. Cossi, G. Scalmani, N. Rega, G.A. Petersson, H. Nakatsuji, M. Hada, M. Ehara, K. Toyota, R. Fukuda, J. Hasegawa, M. Ishida, T. Nakajima, Y. Honda, O. Kitao, H. Nakai, M. Klene, X. Li, J.E. Knox, H.P. Hratchian, J.B. Cross, V. Bakken, C. Adamo, J. Jaramillo, R. Gomperts, R.E. Stratmann, O. Yazyev, A.J. Austin, R. Cammi, C. Pomelli, J.W. Ochterski, P.Y. Ayala, K. Morokuma, G.A. Voth, P. Salvador, J.J. Dannenberg, V.G. Zakrzewski, S. Dapprich, A.D. Daniels, M.C. Strain, O. Farkas, D.K. Malick, A.D. Rabuck, K. Raghavachari, J.B. Foresman, J.V. Ortiz, Q. Cui, A.G. Baboul, S. Clifford, J. Cioslowski, B.B. Stefanov, G. Liu, A. Liashenko, P. Piskorz, I. Komaromi, R.L. Martin, D.J. Fox, T. Keith, M.A. Al-Laham, C.Y. Peng, A. Nanayakkara, M. Challacombe, P.M.W. Gill, B. Johnson, W. Chen, M.W. Wong, C. Gonzalez, and J.A. Pople, Gaussian Inc., Wallingford CT, 2004.
[28] G. Balducci, L. Bencivenni, G. De Rosa, R. Gigli, B. Martine, S.N. Cesaro, J. Mol. Struct. 64 (1980) 163.
[29] M.D. Bruce, G.W. Coates, E. Hauptman, R.M. Waymouth, J.W. Ziller, J. Am. Chem. Soc. 119 (1997) 11174.
[30] (a) M. Knickmeier, G. Erker, T. Fox, J. Am. Chem. Soc. 118 (1996) 9623;
(b) T. Dreier, K. Bergander, E. Wegelius, R. Frohlich, G. Erker, Organometallics 20 (2001) 5067.
[31] F. Nief, F. Mathey, L. Ricard, Organometallics 7 (1988) 921.
[32] J. Tian, G.W. Coates, Angew. Chem., Int. Ed. Engl. 39 (2000) 3626.
[33] J.I. Seeman, Chem. Rev. 83 (1983) 84.
[34] A.B. Pangborn, M.A. Giardello, R.H. Grubbs, R.K. Rosen, F.J. Timmers, Organometallics 15 (1996) 1518.
[35] W. Kuchen, W. Gruenewald, Chem. Ber. 98 (1965) 480.
[36] L.D. Quin, K.A. Mesch, W.L. Orton, Phos. Sulf. Rel. Elem. 12 (1982) 161.
[37] L.E. Manzer, Inorg. Synth. 21 (1982) 135.
[38] SMART Software Reference Manual, Version 5.054, Bruker Analytical X-Ray System Inc., Madison, WI 1997–1998.
[39] SAINTPLUS Software Reference Manual, Version 5.02, Bruker Analytical X-Ray System Inc., Madison, WI 1997–1998.
[40] SHELXTL Software Reference Manual, Version 6.10, December 5th, 2000, Bruker Analytical X-Ray System Inc., Madison, WI.